arXiv:nucl-th/9906010v1 3 Jun 1999

Nucleon-Nucleon Effective Field Theory at NNLO: Radiation Pions and $^1S_0$ Phase Shift[a]

Thomas Mehen and Iain W. Stewart
California Institute of Technology, Pasadena, CA, 91125
E-mail: mehen@theory.caltech.edu, iain@theory.caltech.edu

Low energy phenomena involving two nucleons can be successfully described using effective field theory. Because of the relatively large expansion parameter, it is only at next-to-next-to-leading order (NNLO) where one can expect to see agreement with experiment at the few percent level. The first part of this talk will focus on radiation pion effects, which first appear at NNLO. The power counting for radiation pions is simple for center of mass momentum $p \sim \sqrt{Mm_\pi} \equiv Q_r$, the threshold for pion production. We explain how graphs calculated with the Q_r power counting scale for $p \sim m_\pi$. The Q_r^3 radiation pion contributions to nucleon-nucleon scattering are suppressed by inverse powers of the S-wave scattering lengths. However, we point out that order Q_r^4 radiation contributions might give a NNLO contribution for $p \sim m_\pi$. In the second part of the talk, results for the potential pion and contact interaction part of the NNLO $^1S_0$ phase shift are presented. We emphasize the importance of eliminating spurious poles in the expression for the amplitude at each order in the perturbative expansion. Doing this leaves a total of three free parameters at NNLO. We obtain a good fit to the $^1S_0$ phase shift.

Introduction

This talk focuses on higher order calculations in the low energy effective field theory for two-nucleon systems. In particular, we will be discussing nucleon-nucleon scattering at next-to-next-to-leading order (NNLO) in the expansion recently proposed by Kaplan, Savage and Wise (KSW).[1,2] Observables are expanded in powers of Q/Λ, where Q is either p, the three-momentum of the two nucleons in the center of mass frame, or m_π. Λ is the range of the effective theory. The nuclear S-wave scattering lengths (denoted by a) are very large so that powers of pa have to be summed to all orders at each order of the Q expansion. This requires a novel power counting in which the leading 4-nucleon operator with no derivatives is treated nonperturbatively. To make this power counting manifest in dimensional regularization it is necessary to use subtraction schemes such as PDS[1,2] or OS[3,4], but predictions of the theory are manifestly scheme and scale independent order by order in Q. Higher derivative operators and pion exchange are treated perturbatively.

Various estimates of the range of the theory exist. One estimate comes from examining pion exchange ladder graphs, where each additional loop gives a contribution of order $p \times Mg_A^2/(8\pi f^2) \equiv p/\Lambda_{NN}$, where $\Lambda_{NN} = 300\,\mathrm{MeV}$. Another possibility is that m_ρ or the threshold for Δ production sets the scale for the breakdown of the effective theory, implying a range for S-wave scattering $\sim 700\,\mathrm{MeV}$. It has been suggested [5,6] that two pion exchange contributions to the nucleon-nucleon potential may be become important for momenta of order 400 MeV. These considerations point to a range somewhere between 300 MeV and 700 MeV. Therefore, for $p \sim m_\pi$, the expansion parameter, Q/Λ, is between 1/2 and 1/5. Because the expansion parameter of the theory is rather large, low order calculations in the effective theory cannot be expected to reproduce phase shift data as accurately as potential models with many parameters.

---

[a] CALT-68-2226

Many observables have been computed to NLO in the KSW expansion, including nucleon-nucleon phase shifts,[1,7] Coulomb corrections to proton-proton scattering,[8] electromagnetic form factors of the deuteron,[9] deuteron polarizabilities,[10] proton-proton fusion,[11] $np \to d\gamma$,[12] Compton deuteron scattering,[13] and $\nu d \to \nu d$.[14] Some of these calculations are reviewed in the talk by Martin Savage in this volume.[15] One typically finds errors of order $30-40\%$ at leading order and 10% at NLO. This is consistent with $Q/\Lambda \approx 1/3$, or $\Lambda \approx 400\,\mathrm{MeV}$. This suggests that at NNLO, effective field theory calculations of low energy processes in the two body sector should agree with data at the few percent level, approaching an accuracy comparable to that of potential models. It is for this reason that extending calculations to this order is an important part of the effective field theory program.

In the first half of this talk, we will discuss radiation pion effects, which first appear at NNLO in calculations of nucleon-nucleon scattering. The power counting of KSW has to be modified in the presence of pion radiation because a new scale, $Q_r = \sqrt{Mm_\pi}$, appears.[16] For power counting radiation pions, it is simpler to take $p \sim Q_r$ and count powers of Q_r rather than Q. We give a procedure for determining how a Q_r^n correction scales with Q for $p \sim m_\pi$. The order Q_r^3 radiation pion contribution to nucleon-nucleon scattering turns out to be suppressed by powers of $1/a$. This is actually a consequence of the invariance of the leading order theory under Wigner's $SU(4)$ spin-isospin symmetry.[17] Wigner symmetry is discussed in detail in the talk by Mark Wise in this volume.[18] The order Q_r^4 radiation pion corrections can give an order Q contribution. In the second half of the talk, we present results of a NNLO calculation of nucleon-nucleon scattering in the ${}^1S_0$ channel. It is emphasized that coupling constants of the theory must be treated in a Q expansion. The parameter space is constrained by the requirement that perturbative corrections do not shift the location of the pole in the amplitude and by the solutions of renormalization group equations. Once these constraints are imposed, a three parameter fit to the ${}^1S_0$ phase shift is demonstrated which has $< 2\%$ accuracy at $p \sim m_\pi$ and also reproduces the data well for higher momenta. A similar calculation is discussed in the talk by Gautum Rupak[19,20].

Radiation and Soft Pions

The Lagrangian for the theory of nucleons and pions is

$$\begin{aligned}
\mathcal{L}_\pi &= \frac{f^2}{8}\mathrm{Tr}\,(\partial^\mu\Sigma\,\partial_\mu\Sigma^\dagger) + \frac{f^2\omega}{4}\,\mathrm{Tr}(m_q\Sigma + m_q\Sigma^\dagger) + \frac{ig_A}{2}\,N^\dagger\sigma_i(\xi\partial_i\xi^\dagger - \xi^\dagger\partial_i\xi)N \\
&\quad + N^\dagger\left(iD_0 + \frac{\vec{D}^2}{2M}\right)N - C_0^s(N^T P_i^s N)^\dagger(N^T P_i^s N) \qquad (1) \\
&\quad + \frac{C_2^s}{8}\left[(N^T P_i^s N)^\dagger(N^T P_i^s \overleftrightarrow{\nabla}^2 N) + h.c.\right] \\
&\quad - D_2^s\,\omega\,\mathrm{Tr}(m^\xi)(N^T P_i^s N)^\dagger(N^T P_i^s N) + \ldots\,,
\end{aligned}$$

where operators relevant at NLO are included (and isospin violation is neglected). Here $g_A = 1.25$ is the nucleon axial-vector coupling, $\Sigma = \xi^2$ is the exponential of pion fields, $f = 131\,\mathrm{MeV}$ is the pion decay constant, $m^\xi = (\xi m_q\xi + \xi^\dagger m_q\xi^\dagger)/2$, where $m_q = \mathrm{diag}(m_u, m_d)$ is the quark mass matrix, and $m_\pi^2 = w(m_u + m_d)$. The matrices P_i^s project onto states of definite spin and isospin, and the superscript s denotes the partial wave amplitude mediated by the operator. This talk will be concerned only with S-wave scattering, so $s = S$ (for ${}^1S_0$) or T (for ${}^3S_1$). This notation will be omitted when it is not necessary to distinguish between the two channels.

In the KSW power counting, the C_0 operator is treated nonperturbatively and graphs with a single pion exchange (dressed with C_0 bubbles) first appear at NLO. Loop graphs with pions contain three different kinds of contributions, which are called potential, radiation and soft. The three kinds of pion are characterized by different energy (q_0) and momentum ($\vec{q}$):

$$\begin{array}{ll}
\text{potential} & q_0 \sim \vec{q}^{\,2}/M \\
\text{radiation} & q_0 \sim |\vec{q}| \sim m_\pi \\
\text{soft} & q_0 \sim |\vec{q}| \sim Q_r = \sqrt{M m_\pi}.
\end{array}$$

As stated earlier, when calculating radiation and soft contributions we take $p \sim Q_r$ rather than $p \sim Q$. The three contributions will differ in size and it is necessary to devise a power counting which correctly takes this into account. Before giving the power counting we will illustrate how these contributions arise with a few illustrative examples.

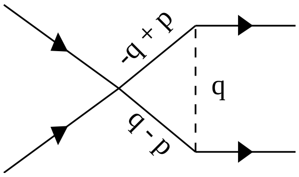

Figure 1: One loop graph with a C_0 and pion that has both potential and radiation contributions

Consider the one loop graph shown in Fig. 1, whose contribution to the amplitude is proportional to

$$\frac{g_A^2 C_0}{2f^2}\int\frac{d^4q}{(2\pi)^4}\,\frac{1}{\frac{E}{2}+q_0-\frac{(\vec{q}-\vec{p})^2}{2M}+i\epsilon}\,\frac{1}{\frac{E}{2}-q_0-\frac{(\vec{q}-\vec{p})^2}{2M}+i\epsilon}\,\frac{\vec{q}^{\,2}}{q_0^2-\vec{q}^{\,2}-m_\pi^2+i\epsilon}$$

When the q_0 integral is performed via contour integration, the integral receives contributions from both pion and nucleon poles. If a nucleon pole is taken then $|q_0| = E/2-(\vec{q}-\vec{p})^2/2M = (2\vec{q}\cdot\vec{p}-\vec{q}^{\,2})/2M$, where in the last step we have used $E=\vec{p}^{\,2}/M$. Since $|\vec{p}|, |\vec{q}| \ll M$, $q_0 \ll |\vec{q}|$, we can expand the pion propagator:

$$\frac{1}{q_0^2-\vec{q}^{\,2}-m_\pi^2} = -\frac{1}{\vec{q}^{\,2}+m_\pi^2}-\frac{q_0^2}{(\vec{q}^{\,2}+m_\pi^2)^2}+\ldots .$$

A pion is referred to as a potential pion whenever the energy dependent piece of its propagator is treated perturbatively. In the KSW power counting, $|\vec{p}| \sim m_\pi \sim \mu_R \sim |\vec{q}| \sim Q$. Each nucleon propagator gives a factor of M/Q^2 since $E \sim q_0 \sim Q^2/M$. The measure $d^4q \sim Q^5/M$, and in a scheme with manifest power counting, $C_0 \sim 1/(M\mu_R) \sim 1/(MQ)$. Using this counting it is straightforward to see that this graph is order Q^0, i.e., it is a NLO contribution. The first correction from the expansion in $q_0^2/(\vec{q}^{\,2}+m_\pi^2)$ is suppressed relative to the leading potential contribution by Q^2/M^2, and so is N^{3}LO.

There is also a contribution from the pion pole. In this case $q_0^2 = \vec{q}^{\,2}+m_\pi^2$. In the nucleon propagators, the factors of $(2\vec{q}\cdot\vec{p}-\vec{q}^{\,2})/2M \ll q_0$ and must be treated perturbatively. With the KSW power counting, the nucleon propagators in the graph in Fig. 1 are $\pm 1/q_0 \sim 1/Q$, and the loop measure scales as Q^4, so the graph is $\sim Q$. Therefore, this radiation pion contribution first appears at NNLO.

While KSW power counting works for the graph in Fig. 1, it fails for other graphs with radiation pions. As an example, consider the graph in Fig. 2 which

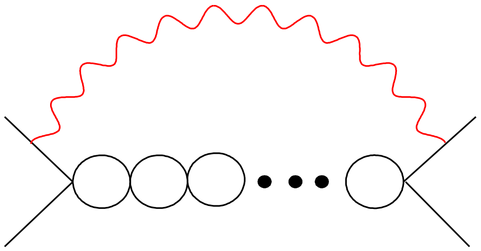

Figure 2: A radiation pion graph with n internal C_0 bubbles.

contains n nucleon bubbles inside a radiation pion loop. The loop integral in this graph vanishes if the pion pole is not taken so there is no potential pion contribution. Emission of the radiation pion in these graphs changes the spin/isospin of the nucleon pair. Therefore, if the external nucleons are in a spin-triplet (singlet) state, then the coefficients appearing in the internal bubble sum are C_0^S (C_0^T). For definiteness, consider nucleon-nucleon scattering in the ${}^1S_0$ channel. The contribution from the graph in Fig. 2 is:

$$\frac{g_A^2}{2f^2}\int\frac{d^4q}{(2\pi)^4}\,\frac{i}{q_0+i\epsilon}\,\frac{i}{q_0+i\epsilon}\,\frac{-i\,\vec{q}^{\,2}}{q_0^2-\vec{q}^{\,2}-m_\pi^2+i\epsilon}[-iC_0^T(\mu_R)]^{n+1}$$
$$\times\left[\int\frac{d^4k}{(2\pi)^4}\,\frac{i}{q_0-k_0+\frac{E}{2}-\frac{(\vec{k}-\vec{q})^2}{2M}+i\epsilon}\,\frac{i}{k_0+\frac{E}{2}-\frac{\vec{k}^2}{2M}+i\epsilon}\right]^n .$$

The q_0 integral is closed around the one pion pole above the real axis so $q_0 \sim |\vec{q}\,| \sim Q$. In the k_0 integrals a nucleon pole must be taken. In the KSW power counting, $k_0 \sim Q^2/M, |\vec{k}\,| \sim Q$. The graph then scales as $(Q/M)^{n+1}$. This suggests that graphs with nucleon bubbles inside the radiation loop are suppressed relative to the one loop radiation pion graph. However, explicitly performing the q_0 and k_0 integrals gives

$$-\,iC_0^T(\mu_R)\,\frac{g_A^2}{2f^2}\int\frac{d^3q}{(2\pi)^3}\,\frac{\vec{q}^{\,2}}{(\vec{q}^{\,2}+m_\pi^2)^{3/2}}\left[\int\frac{d^3k}{(2\pi)^3}\,\frac{-MC_0^T(\mu_R)}{\vec{k}^{\,2}+M(\vec{q}^{\,2}+m_\pi^2)^{1/2}-ME}\right]^n .$$

The size of the loop momenta k in the nucleon bubbles is $\sim \sqrt{Mm_\pi}$ even for $p < \sqrt{Mm_\pi}$. The integral will be dominated by $\vec{q} \sim m_\pi$ so the graph will scale as

$$\frac{1}{\Lambda_\chi^2}\,\frac{m_\pi^2}{M\mu_R}\left(\frac{\sqrt{Mm_\pi}}{\mu_R}\right)^n .$$

(Recall $\Lambda_\chi = 4\pi f$). For $\mu_R \sim Q \sim m_\pi$, we see that graphs with additional bubbles are enhanced, contrary to the KSW power counting. The sum over graphs with an arbitrary number of bubbles is μ_R independent and the correct estimate for the size is obtained when $\mu_R \sim \sqrt{Mm_\pi}$. At this scale, these graphs and their sum are of order $m_\pi^{3/2}/(M^{3/2}\Lambda_\chi^2) = Q_r^3/(M^3\Lambda_\chi^2)$.

In the KSW power counting, one assumes the loop momentum in the nucleon bubbles is dominated by $k \sim Q, k_0 \sim Q^2/M$. However, when the nucleon bubbles are inside a radiation pion loop, the energy flowing into the nucleon bubbles is actually order m_π, and therefore $k^0 \sim m_\pi$ and $k \sim \sqrt{Mm_\pi} \equiv Q_r$. This scale corresponds to the threshold for on-shell pion production.

In general, radiation pion graphs will depend on p, m_π and M in a complicated way, making them difficult to power count if one takes $p \sim m_\pi$. However, the natural scale for loop momenta with radiation pions is Q_r, and the power counting simplifies considerably if we consider nucleons scattering at $p \sim Q_r$. Later we will discuss what happens as p is lowered back down to m_π.

Power counting at the scale Q_r is straightforward. We take $p \sim \mu_R \sim Q_r$. The C_{2n} scale with μ_R exactly the same way as in the KSW power counting, $C_{2n}p^{2n} \sim p^{2n}/\mu_R^{n+1} \sim Q_r^{n-1}$. A radiation pion propagator gives M^2/Q_r^4, the pion nucleon coupling gives Q_r^2/M. Nucleon propagators scale like M/Q_r^2. In a radiation loop $q_0 \sim |\vec{q}| \sim m_\pi$, so the loop measure $d^4q \sim Q_r^8/M^4$. The measure of a potential loop scales as Q_r^5/M. Using this power counting it is straightforward to show that all graphs with one radiation pion and an arbitrary number of C_0's scale as $Q_r^3/(M^3\Lambda_\chi^2)$. These graphs are shown in Fig. 3.

It is interesting to examine the result of evaluating some of the diagrams in Fig. 3 explicitly[16] ($\bar{\mu}^2 = \mu^2\pi e^{-\gamma_E}$):

$$\begin{aligned}
a) &= -3i\mathcal{A}_{-1}\frac{g_A^2 m_\pi^2}{(4\pi f)^2}\left[\frac{1}{\epsilon}+\frac{1}{3}-\ln\left(\frac{m_\pi^2}{\bar{\mu}^2}\right)\right], \qquad (2)\\
b) &= [\mathcal{A}_{-1}]^2\,\frac{g_A^2 M m_\pi^2}{(4\pi f)^2}\left\{\frac{3\,p}{4\pi}\left[\frac{1}{\epsilon}+\frac{7}{3}-2\ln 2-\ln\left(\frac{m_\pi^2}{\bar{\mu}^2}\right)-\ln\left(\frac{-p^2}{\bar{\mu}^2}\right)\right]\right.\\
&\qquad\left.+\frac{i\sqrt{Mm_\pi}}{4\sqrt{\pi}}\,I_1\left(\frac{E}{m_\pi}\right)\right\},\\
c) &= \frac{ig_A^2}{\sqrt{\pi}f^2}\left(\frac{m_\pi}{M}\right)^{3/2} I_2\left(\frac{E}{m_\pi}\right).
\end{aligned}$$

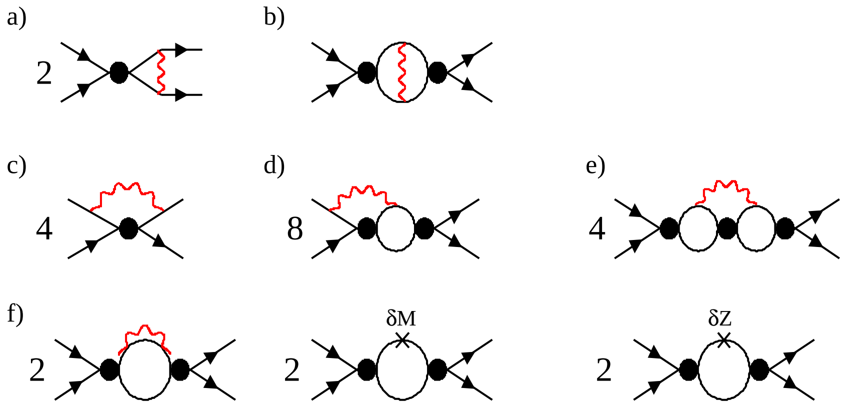

Figure 3: Leading order radiation pion graphs for NN scattering. The solid lines are nucleons, the wavy lines are radiation pions and δM, δZ are the mass and field renormalization counterterms. The filled dot denotes the $C_0(\mu_R)$ bubble chain. There is a further field renormalization contribution that is not shown, but is included in the calculation.[16]

I_1 and I_2 are hypergeometric functions. The $1/\epsilon$ poles are cancelled by insertions of a $D_2 m_\pi^2$ counterterm. The leading order amplitude

$$\mathcal{A}_{-1} = -\frac{4\pi}{M}\frac{1}{1/a^S + ip}\,,$$

scales as $\sim 1/(Mp)$, so we see that Eq. (2) has terms proportional to

$$\left(\frac{m_\pi}{M}\right)^{3/2}, \qquad \frac{m_\pi^2}{Mp} \qquad \text{and} \qquad \frac{m_\pi^{5/2}}{M^{1/2}p^2}\,.$$

For $p \sim Q_r$ these terms scale as Q_r^3/M^3, as anticipated by the power counting. At $p \sim m_\pi \sim Q$, these terms scale like $(Q/M)^{3/2}, Q/M$, and $(Q/M)^{1/2}$ respectively. Bubble sums which do not appear inside radiation loops will be referred to as external bubble sums. These bubble sums are responsible for the factors of p in the denominators, and thus the enhancement of some terms at low momentum. Graphs with two external bubble sums have terms that are enhanced by $Q_r^2/Q^2 \sim 1/m_\pi$ (and $Q_r/Q \sim 1/\sqrt{m_\pi}$), while graphs with one external bubble sum have terms enhanced by $1/\sqrt{m_\pi}$. Individual graphs like b) have parts that scale differently with Q. Terms which scale like $Q^{1/2}$ at low p are actually larger than NNLO in the Q counting. The $Q^{1/2}$ contributions come from graphs $b), e)$ and $f)$, and cancel when the graphs are added together. Presently it is not known whether this cancellation occurs for some reason or is merely an accident.

The sum of all Q_r^3 graphs is:

$$
\begin{aligned}
i\,\mathcal{A}^{rad} &= 6i\,\mathcal{A}_{-1}^2 \frac{g_A^2 m_\pi^2}{(4\pi f)^2}\,\frac{M}{4\pi}\left(\frac{1}{a^S}-\frac{1}{a^T}\right)\left[\kappa+\ln\!\Big(\frac{\mu^2}{m_\pi^2}\Big)\right] \\
&\quad + i\,\mathcal{A}_{-1}^2\left(\frac{M}{4\pi}\right)^2\left(\frac{1}{a^S}-\frac{1}{a^T}\right)^2 \frac{g_A^2}{\sqrt{\pi} f^2}\Big(\frac{m_\pi}{M}\Big)^{3/2} I_2\Big(\frac{E}{m_\pi}\Big)\,, \qquad (3)
\end{aligned}
$$

where the $\ln(\mu)$ dependence is cancelled by $D_2(\mu)$. (For the ${}^3S_1$ channel, the result is the same as above with $a_S \leftrightarrow a_T$.) The final answer turns out to be much smaller than anticipated by the power counting. For $p \sim Q_r$, the first term is suppressed by a factor of $1/Q_r(1/a^S - 1/a^T)$, the second by $1/Q_r^2(1/a^S - 1/a^T)^2$. This suppression occurs because the radiation pions couple to a charge of Wigner's $SU(4)$, which is a symmetry of the leading order Lagrangian in the limit $a_S, a_T \to \infty$ (or $a_S = a_T$).[17,18] The order Q_r^3 radiation pion graphs are a tiny correction to the S-wave scattering amplitude.

The next important radiation pion contribution comes from graphs with one insertion of a C_2p^2, $D_2m_\pi^2$, or G_2 operator [4] or a potential pion, and one radiation pion with an arbitrary number of C_0's. Power counting these graphs gives $Q_r^4/(M^3\Lambda_\chi^2\Lambda)$, i.e. these are suppressed by Q_r/Λ relative to the leading radiation pion graphs in Fig. 3. Note that $Q_r = 360\,\mathrm{MeV}$, so for the most pessimistic estimates of Λ, the Q_r/Λ expansion does not converge. If this is the case then the radiation pion contribution is incalculable. This is true of radiation contributions even when we scale down to $p \sim m_\pi$. However, at the low momenta where the theory would be applicable, the radiation pions could be integrated out. For example, the hypergeometric function $I_2(E/m_\pi) = I_2(p^2/(Mm_\pi))$ could be expanded in a series in p^2 and the effect of each term absorbed[b] into the definition of a C_{2n}. Assuming the radiation pion contribution is computable, the Q_r^4 correction is almost certainly larger than the Q_r^3 correction. Since the C_2p^2, $D_2m_\pi^2$ operators and potential pion exchange do not respect Wigner's $SU(4)$, there will be no suppression by factors of $1/(a\,Q_r)$.

An important issue which needs to be addressed is how the radiation pions graphs scale as p is lowered from Q_r to m_π. We saw that the Q_r^3 graphs had pieces that scaled as $Q^{1/2}, Q, Q^{3/2}, \ldots$, for $p \sim m_\pi$, and that this enhancement can be understood by counting the number of external bubble sums. In order to know which radiation pion graphs to include at a given order in the KSW power counting, we must know how a Q_r^n correction scales with Q for $p \sim m_\pi$. It turns out that an order Q_r^n calculation is sufficient to determine the order $Q^{n/2-1}$ result.

---

[b] Unfortunately, the resulting theory below the scale Q_r would no longer respect chiral symmetry. Operators involving a different number of pion fields could have different coefficients.

To see this first consider the Q expansion of $p\cot\delta$:

$$\begin{aligned} p\cot\delta &= ip + \frac{4\pi}{M}\frac{1}{\mathcal{A}} \\ &= ip + \frac{4\pi}{M}\frac{1}{\mathcal{A}_{-1}} - \frac{4\pi}{M}\frac{\mathcal{A}_0}{\mathcal{A}_{-1}^2} - \frac{4\pi}{M}\left(\frac{\mathcal{A}_1}{\mathcal{A}_{-1}^2} - \frac{\mathcal{A}_0^2}{\mathcal{A}_{-1}^3}\right) \\ &\quad - \frac{4\pi}{M}\left(\frac{\mathcal{A}_2}{\mathcal{A}_{-1}^2} - \frac{2\mathcal{A}_0\mathcal{A}_1}{\mathcal{A}_{-1}^3} + \frac{\mathcal{A}_0^3}{\mathcal{A}_{-1}^4}\right) + \ldots . \end{aligned}$$

$p\cot\delta$ is real and an analytic function of p^2 near $p=0$. This will be true order by order in Q so:

$$\begin{aligned} \frac{\mathcal{A}_0}{\mathcal{A}_{-1}^2} &= f_0 \;\Rightarrow\; \mathcal{A}_0 = f_0\mathcal{A}_{-1}^2\,, \\ \frac{\mathcal{A}_1}{\mathcal{A}_{-1}^2} - \frac{\mathcal{A}_0^2}{\mathcal{A}_{-1}^3} &= f_1 \;\Rightarrow\; \mathcal{A}_1 = f_1\mathcal{A}_{-1}^2 + f_0^2\mathcal{A}_{-1}^3\,, \\ \frac{\mathcal{A}_2}{\mathcal{A}_{-1}^2} - \frac{2\mathcal{A}_0\mathcal{A}_1}{\mathcal{A}_{-1}^3} + \frac{\mathcal{A}_0^3}{\mathcal{A}_{-1}^4} &= f_2 \;\Rightarrow\; \mathcal{A}_2 = f_2\mathcal{A}_{-1}^2 + 2f_0f_1\mathcal{A}_{-1}^3 + f_0^3\mathcal{A}_{-1}^4\,, \end{aligned}$$

where the f_n are real functions of p which are analytic about $p^2=0$. We see that the general form of a higher order amplitude is powers of $\mathcal{A}_{-1}$ multiplied by functions of p. The crucial point is that the function multiplying the $\mathcal{A}_{-1}^2$ is the only new contribution. The coefficient of $\mathcal{A}_{-1}^n, n>2$, is determined by lower order amplitudes. In the Q expansion of $p\cot\delta$ the latter contributions will cancel.

This generalizes to the Q_r expansion of radiation pion graphs, the only difference being that the radiation pion contribution starts out at Q_r^3, while the potential pion starts out at Q_r^0. A Q_r^n radiation pion correction to the amplitude will be of the form:

$$\mathcal{A}_n = \mathcal{A}_{-1}^2 f_{n,2} + \mathcal{A}_{-1}^3 f_{n,3} + \ldots + \mathcal{A}_{-1}^{n-1} f_{n,n-1}.$$

Again, the $f_{n,m}$ are analytic about $p^2=0$ and all the $f_{n,m}$ except for $f_{n,2}$ will be determined from lower order amplitudes. Since $\mathcal{A}_n \sim Q_r^n$ and $\mathcal{A}_{-1} \sim 1/(Mp)$, $f_{n,m} \sim Q_r^{n+m}$ for $p \sim Q_r$. To understand how $f_{n,m}$ scales with Q as p is lowered to m_π, note that without loss of generality, $f_{n,m}$ can be written as

$$f_{n,m} = \frac{(\sqrt{Mm_\pi})^{n+m}}{\Lambda_\chi^2\,\overline{\Lambda}^{\,n-m}}\hat{f}_{n,m}\left(\frac{p}{\sqrt{Mm_\pi}},\ldots\right)\,,$$

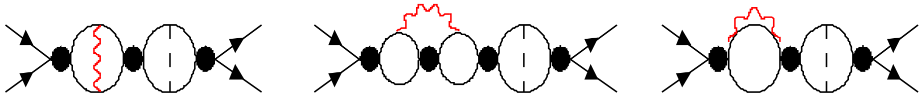

Figure 4: Example of order Q_r^4 graphs that have three external bubble sums.

where the ellipses denote momentum dependence that involves scales other than Q_r, and $\overline{\Lambda} = \Lambda_\chi$, Λ, or M. For $p \sim m_\pi$ the ellipse denote dependence on the dimensionless variables p/m_π, pa, and $p/\overline{\Lambda}$. For $p \sim m_\pi$, $p/\sqrt{M m_\pi} \sim (Q/M)^{1/2}$ and the function $\hat{f}_{n,m}$ can be expanded in its first argument:

$$\mathcal{A}_{-1}^m f_{n,m} = \mathcal{A}_{-1}^m \frac{(\sqrt{M m_\pi})^{n+m}}{\Lambda_\chi^2 \ \overline{\Lambda}^{n-m}} \hat{f}_{n,m}\left(0, \ldots\right) \left[1 + O\left(\frac{Q}{M}\right)^{1/2}\right] .$$

The leading term scales as $\sim Q^{n/2-m/2}$ for $p \sim m_\pi \sim Q$. Since only the $m = 2$ term actually ends up contributing to $p \cot\delta$, the new contribution at Q_r^n scales like $Q^{n/2-1}$ (plus subleading terms) for $p \sim m_\pi$. This is consistent with the result of the Q_r^3 calculation, where the largest contributions from individual graphs scaled as $Q^{1/2}$. A cancellation between graphs resulted in this contribution vanishing. The remaining terms scale as Q, $Q^{3/2}, \ldots$ (counting $1/a \sim Q$). The Q_r^n radiation pion contribution could have a $Q^{1/2}$ contribution from the $\mathcal{A}_{-1}^{n-1} f_{n,n-1}$ term. But this contribution is determined by the Q_r^3 amplitude which vanished; so there will be no $Q^{1/2}$ contribution from any radiation pion graph. For example, at Q_r^4 the terms proportional to $\mathcal{A}_{-1}^3$ comes from graphs such as those shown in Fig. 4. These graphs factorize into two pieces which are lower order and it is easy to see that the same cancellation between the $Q^{1/2}$ pieces of the graphs $b), e)$ and $f)$ will also occur at Q_r^4.

Since $Q^{n/2-1} = Q$ for $n = 4$, the Q_r^4 radiation pion graphs may have a contribution that is NNLO for $p \sim m_\pi$. We have checked that graphs with one insertion of the $D_2 m_\pi^2$ operator do not give rise to such a contribution, but a calculation of the remaining Q_r^4 graphs has not been performed. These graphs need to be computed in order to obtain the complete NNLO amplitude. Unfortunately, graphs with one potential and one radiation pion are numerous. Higher Q_r^n amplitudes may have a contribution which scales as Q for $p \sim m_\pi$ from the $\mathcal{A}_{-1}^{n-2} f_{n,n-2}$ term. But these will cancel in the Q expansion of $p \cot\delta$. Note that a calculation of the order Q_r^5 graphs would be necessary to determine the order $Q^{3/2}$ terms.

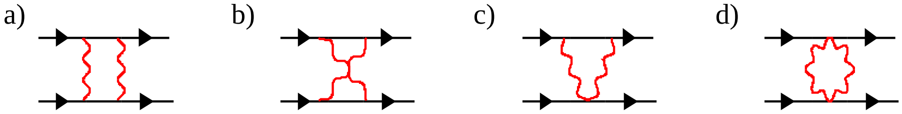

Figure 5: Examples of one-loop graphs which have soft pion contributions. Graphs a)-d) also have a radiation pion contribution, while in addition graph a) has a potential pion contribution.

Finally, we briefly discuss soft contributions. These first arise in box-type diagrams with two pions, such as those shown in Fig. 5. Dressing these graphs on the outside with C_0 bubbles gives further diagrams of the same order. Unlike radiation graphs, which are dominated by loop momenta $|\vec{q}| \sim m_\pi$, the box-like diagrams receive nonvanishing contributions from $|\vec{q}| \sim Q_r$. It is this latter type of contribution which is called soft. In soft loops the measure $d^4q \sim Q_r^4$ instead of Q_r^8/M^4. For nucleon propagators in soft loops, the loop energy is always greater than the nucleon's kinetic energy, so the propagator is static (like heavy quark effective theory propagators, see [21] or [22]). These propagators scale as $1/Q_r$. Pion propagators scale as $1/Q_r^2$ and pion-nucleon vertices give a factor of Q_r. Power counting the graphs in Fig. 5 gives $\sim Q_r^2$ for the soft contribution and $\sim Q_r^4/M^2$ for the radiation contribution. The contribution from each regime can be separated using the method of asymptotic expansions [23,24,25] and explicit evaluation [16] of the graphs verifies the power counting appropriate for each type of contribution. At $p \sim Q_r$, the soft contribution actually dominates all radiation pion graphs we have considered so far. However, for $p \sim m_\pi$ these soft graphs are order Q^2, and therefore are not enhanced by the scaling down to $p \sim m_\pi$. The leading order soft graphs are N^{3}LO in the KSW power counting.

NNLO Calculation of the $^1S_0$ Phase Shift[c]

In this section, we present a partial NNLO calculation of the $^1S_0$ phase shift. A more detailed analysis will be given in a future publication.[26] The first piece of the Q_r^3 radiation pion contribution in Eq. (3) is order Q. The second term is order $Q^{3/2}$ and is not included in the NNLO calculation. The relativistic corrections are computed in Ref.[27] and shown to be negligible. This is because they are suppressed relative to the leading order amplitude by $(Q/M)^2$ rather than $(Q/\Lambda)^2$ and so are smaller than other NNLO corrections. The calculation here includes order Q contact interactions and potential pion graphs. The NNLO calculation is incomplete because of the omission of the Q_r^4 radiation pion graphs, as discussed in the previous section. The pieces of the NNLO amplitude which are included are expected to scale as $Q/(M\Lambda^2)$ while the Q_r^4 radiation pion graphs are expected to scale as $Q/(\Lambda_\chi^2\Lambda)$ for $p \sim m_\pi$. Since $\Lambda < \Lambda_\chi \approx M$, the contribution from Q_r^4 radiation pion graphs may be smaller than what has been included.

---

[c] The work presented in this section was done in collaboration with Sean Fleming.

Since we are only interested in the ${}^1S_0$ channel, only $s = S$ operators are relevant and this superscript will be omitted in the following discussion. At NNLO, the following terms are added to the Lagrangian in Eq. (1):

$$\begin{aligned}\mathcal{L} = -\frac{C_4}{64}&\left[(N^T P_i N)^\dagger (N^T P_i \overset{\leftrightarrow}{\nabla}{}^4 N) + h.c. + 2(N^T P_i \overset{\leftrightarrow}{\nabla}{}^2 N)^\dagger (N^T P_i \overset{\leftrightarrow}{\nabla}{}^2 N)\right] \\ &+\frac{E_4}{8}\omega \mathrm{Tr}(m^\xi)\left[(N^T P_i N)^\dagger (N^T P_i \overset{\leftrightarrow}{\nabla}{}^2 N) + h.c.\right] \\ &-\frac{D_4}{2}\omega^2\left\{\mathrm{Tr}^2(m^\xi) + 2\mathrm{Tr}[(m^\xi)^2]\right\}(N^T P_i N)^\dagger (N^T P_i N)\,, \end{aligned} \tag{4}$$

where only terms relevant for the phase shift are included and isospin violation is neglected. All calculations presented in this section will be done in the PDS renormalization scheme[1,2] with spin and isospin traces done in four dimensions.

There are six coefficients that appear at NNLO: C_0, which is present in the leading order calculation, C_2 and D_2, which first appear at NLO, and C_4, E_4, and D_4. It is important that the coupling constants are expanded in Q: [3]

$$\begin{aligned} C_0 &\to C_0 + C_{0,0} + C_{0,1} \\ C_2 &\to C_2 + C_{2,-1} \\ D_2 &\to D_2 + D_{2,-1}\,. \end{aligned} \tag{5}$$

The first piece of C_0 is treated nonperturbatively (i.e. $C_0 \sim Q^{-1}$), while $C_{0,0} \sim Q^0, C_{0,1} \sim Q$. Solving the renormalization group equations (RGE) for the couplings perturbatively ensures that the amplitude is μ independent order by order in the expansion. Therefore, theoretical expressions for physical quantities, such as the scattering length or the location of the pole, are always μ independent. Physically, the Q expansion of the couplings is a consequence of the fact that higher order loop graphs with pions can renormalize the short distance operators at different orders in Q, and therefore different values of the couplings will be obtained at different orders in the expansion.

When a coupling is expanded in Q and its RGE solved perturbatively, a new constant of integration is obtained for each term in the expansion. For example, the RGE for C_0 is:

$$\mu\frac{\partial}{\partial\mu}C_0 = \frac{M\mu}{4\pi}\left(C_0 + \frac{g_A^2}{2f^2}\right)^2 . \tag{6}$$

After the perturbative expansion of C_0 this becomes

$$\mu\frac{\partial}{\partial\mu}C_0 = \frac{M\mu}{4\pi}C_0^2\,, \qquad \mu\frac{\partial}{\partial\mu}C_{0,0} = 2\frac{M\mu}{4\pi}C_0\left(C_{0,0} + \frac{g_A^2}{2f^2}\right),$$
$$\mu\frac{\partial}{\partial\mu}C_{0,1} = \frac{M\mu}{4\pi}\left[2\,C_0\,C_{0,1} + \left(C_{0,0} + \frac{g_A^2}{2f^2}\right)^2\right],$$

with solutions

$$C_0 = \frac{4\pi}{M}\frac{1}{-\mu+\gamma}\,, \qquad C_{0,0} = \frac{M\kappa}{4\pi}\,C_0^2 - \frac{g_A^2}{2f^2}\,,$$
$$C_{0,1} = \frac{1}{C_0}\left(C_{0,0} + \frac{g_A^2}{2f^2}\right)^2 + \frac{M\kappa'}{4\pi}\,C_0^2\,. \tag{7}$$

Three constants of integration appear: γ, κ and κ'; one for each term in the Q expansion of C_0. For consistency we must assign these constants a Q counting. For instance, $C_{0,0}$ has a term in its solution $\kappa\, C_0^2 \sim \kappa/\mu^2$. Since $C_{0,0} \sim Q^0$, κ must be of order Q^2. This reflects the fact that κ is intrinsically small. In the theory without pions, $\kappa = \gamma - 1/a$. As we will see below, the values of γ, κ, κ' may be fixed by demanding that the amplitude has the correct pole structure. In this case, $\kappa \approx r_0/(2a^2) \sim Q^2$. The results in Eq. (7) can also be obtained by solving Eq. (6) exactly and expanding the result (including the constant of integration) in Q. Because of the perturbative expansion of the couplings in Eq. (5) there are ten constants of integration at NNLO. However, the NNLO amplitude will depend only on six independent linear combinations of these constants. There are two further constraints on the number of free parameters: 1) at this order, C_4, E_4 and D_4 are determined entirely in terms of lower order couplings; 2) spurious double and triple poles in the NLO and NNLO amplitudes must be cancelled in order to obtain a good fit.

The fact that C_4, E_4 and D_4 are determined in terms of lower order couplings is a consequence of solving the RGE's and applying the KSW power counting. For instance[2], the RGE for C_4 is:

$$\mu\frac{\partial}{\partial\mu}C_4 = \frac{M\mu}{4\pi}\left(2\,C_0\,C_4 + C_2^2\right),$$

which has the solution

$$C_4 = \frac{C_2^2}{C_0} + \rho \frac{M}{4\pi} C_0^2 \,,$$

where ρ is a constant of integration. In the theory without pions, ρ is proportional to the shape parameter, which is $\sim Q^0$ in the KSW power counting. It is also reasonable to consider $\rho \sim Q^0$ in the theory with pions, since ρ is a constant of integration in the RGE for the lowest order term in the Q expansion of C_4. Therefore, $C_2^2/C_0 \sim Q^{-3}$, while $\rho C_0^2 M/(4\pi) \sim Q^{-2}$. The second term is subleading in the Q expansion, and should be omitted at NNLO, so $C_4 = C_2^2/C_0$. Similar relations for E_4, D_4 hold at NNLO:

$$E_4 = \frac{2 C_2 D_2}{C_0} \,, \qquad D_4 = \frac{D_2^2}{C_0} \,.$$

It is interesting to note that these relations arise even though there are $\ln(\mu^2)$ terms in the amplitude which contribute to the beta functions for E_4 and D_4.

Because of the nonperturbative treatment of C_0, spurious poles arise at higher orders in the expansion. The leading order amplitude $\mathcal{A}_{-1}$ has a simple pole at $p = i\gamma$. The NLO calculation is proportional to $\mathcal{A}_{-1}^2$, and therefore has a double pole, while the NNLO amplitude has terms proportional to $\mathcal{A}_{-1}^2$ and $\mathcal{A}_{-1}^3$. To obtain a good fit at low momentum, parameters need to be fixed so that the amplitude has only a simple pole at each order in the expansion. This requires that $\mathcal{A}_{-1}$ have its pole in the correct location and that the residues of the spurious double and triple poles vanish. This requirement leads to the following good fit conditions: [3]

$$\left. \frac{1}{\mathcal{A}_{-1}} \right|_{p=p^*} = 0 \,, \qquad \left. \frac{\mathcal{A}_0}{\mathcal{A}_{-1}^2} \right|_{p=p^*} = 0 \,, \qquad \left. \frac{\mathcal{A}_1}{\mathcal{A}_{-1}^2} \right|_{p=p^*} = 0 \,, \tag{8}$$

where p^* is the location of the physical pole. The second condition first appears at NLO, the third at NNLO. The residue of the triple pole in $\mathcal{A}_1$ is cancelled by the second equation in Eq. (8). The first equation results in $\gamma = -ip^*$, while the other equations give constraints which eliminate two of the remaining parameters. Eq. (8) will also apply in the ${}^3S_1$ channel.

The graphs evaluated in the NNLO calculation are shown in Fig. 6. The final result is surprisingly simple. The amplitude up to NNLO is:

$$\mathcal{A}_{-1} = -\frac{4\pi}{M} \frac{1}{\gamma + ip} \,,$$

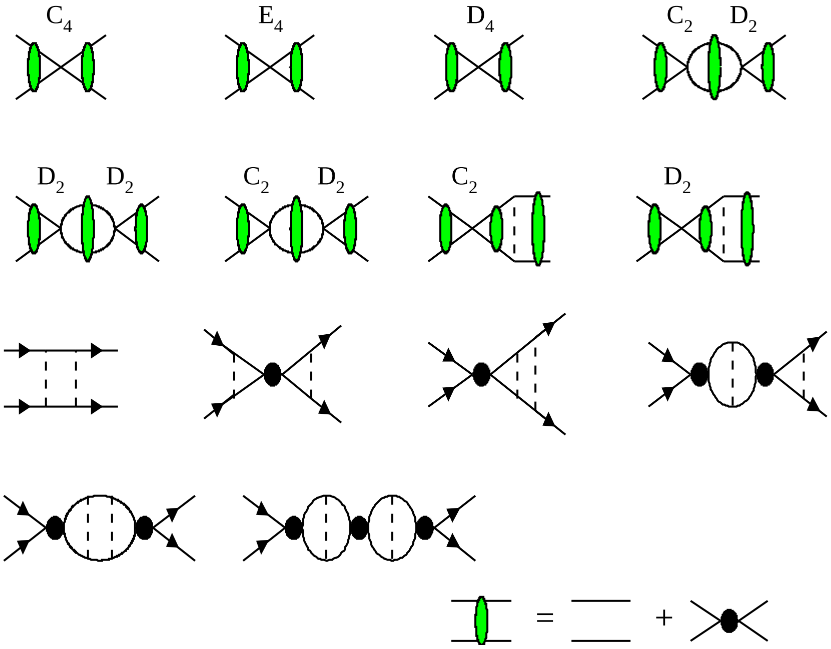

Figure 6: Order Q contact interaction and potential pion graphs for the ${}^1S_0$ channel. The shaded circle denotes a C_0 bubble sum. At this order the first six graphs cancel each other as explained in the text.

$$
\begin{aligned}
\mathcal{A}_0 = & -\mathcal{A}_{-1}^2(\zeta_1\, p^2 + \zeta_2\, m_\pi^2) \\
& + \frac{g_A^2}{2f^2}\mathcal{A}_{-1}^2\Big(\frac{M m_\pi}{4\pi}\Big)^2\left[\frac{(\gamma^2-p^2)}{4p^2}\ln\Big(1+\frac{4p^2}{m_\pi^2}\Big) - \frac{\gamma}{p}\tan^{-1}\left(\frac{2p}{m_\pi}\right)\right], \\
\mathcal{A}_1 = & \frac{\mathcal{A}_0^2}{\mathcal{A}_{-1}} - \mathcal{A}_{-1}^2\Big(\zeta_3\, m_\pi^2 + \zeta_4\, p^2 + \zeta_5\frac{p^4}{m_\pi^2}\Big) + \mathcal{A}_0\frac{M g_A^2}{8\pi f^2}\,\frac{m_\pi^2}{p}\left[\frac{\gamma}{2p}\,\ln\Big(1+\frac{4p^2}{m_\pi^2}\Big)\right. \\
& \left. -\tan^{-1}\Big(\frac{2p}{m_\pi}\Big)\right] + \frac{M\mathcal{A}_{-1}^2}{4\pi}\Big(\frac{M g_A^2}{8\pi f^2}\Big)^2\frac{m_\pi^4}{4p^3}\left\{2(\gamma^2-p^2)\,\mathrm{Im}\,\mathrm{Li}_2\Big(\frac{-m_\pi}{m_\pi-2ip}\Big)\right. \\
& -4\gamma\, p\,\mathrm{Re}\,\mathrm{Li}_2\Big(\frac{-m_\pi}{m_\pi-2ip}\Big) - \frac{\gamma\, p\,\pi^2}{3} - (\gamma^2+p^2)\left[\mathrm{Im}\,\mathrm{Li}_2\Big(\frac{m_\pi+2ip}{-m_\pi+2ip}\Big)\right. \\
& \left.\left. +\frac{\gamma}{4p}\ln^2\left(1+\frac{4p^2}{m_\pi^2}\right) - \tan^{-1}\left(\frac{2p}{m_\pi}\right)\ln\left(1+\frac{4p^2}{m_\pi^2}\right)\right]\right\}.
\end{aligned}
\tag{9}
$$

Using this amplitude it is easy to verify that the S-matrix is unitary to the order we are working. The six linearly independent constants appearing in the amplitude are $\gamma, \zeta_1, \zeta_2, \zeta_3, \zeta_4, \zeta_5$. By definition $\zeta_1 - \zeta_5$ are dimensionless. They are given in terms of coupling constants in the Appendix.

For the ${}^1S_0$ channel, the location of the pole is determined by solving

$$-\frac{1}{a} + \frac{r_0}{2}(p^*)^2 - ip^* = 0\,. \tag{10}$$

Adding the shape parameter correction to Eq. (10) changes the location of the pole by less than 0.01%, so this approximation for the physical pole location is sufficiently accurate. Eq. (10) has a solution for $p^* = -i\,7.877\,\mathrm{MeV}$, which fixes the single LO parameter, $\gamma = -7.877\,\mathrm{MeV}$. The NLO good fit condition relates the constants ζ_1 and ζ_2,

$$\begin{aligned} &-\zeta_1\gamma^2 \;+\; \zeta_2 m_\pi^2 + \frac{M m_\pi^2}{4\pi}\frac{g_A^2 M}{8\pi f^2}\left[\frac{1}{2}\log\left(1 - \frac{4\gamma^2}{m_\pi^2}\right) - \tanh^{-1}\left(\frac{2\gamma}{m_\pi}\right)\right] = 0 \\ &\qquad \Rightarrow \zeta_2 = \frac{\gamma^2}{m_\pi^2}\,\zeta_1 + \frac{M}{4\pi}\frac{g_A^2 M}{8\pi f^2}\left[-\frac{2\gamma}{m_\pi} - \frac{2\gamma^2}{m_\pi^2} + \mathcal{O}\Big(\frac{\gamma^3}{m_\pi^3}\Big)\right]\,. \end{aligned} \tag{11}$$

We can use this equation to eliminate ζ_2 in favor of ζ_1, leaving one new parameter in the fit at NLO. This good fit condition gives non-trivial m_π dependence to the perturbative contributions to C_0 (such as κ) as emphasized in Refs.[28,19,6]. ζ_1 is fixed by doing a weighted least squares fit to low momentum data. Note that ζ_1 appears in the good fit condition multiplied by γ^2. Therefore, the value of ζ_2 is insensitive to the value of ζ_1 obtained from the fitting procedure. To a good degree of accuracy we can ignore ζ_1 in Eq. (11), and then we find $\zeta_2 \approx 0.03$. ζ_2 is small because it is proportional to γ/m_π.

At NNLO, $\zeta_5 = 0$ once we impose $C_4 = C_2^2/C_0$. The condition in Eq. (11) must still be satisfied. The NNLO good fit condition involves ζ_3 and ζ_4,

$$\begin{aligned} \zeta_3 &= \frac{\gamma^2}{m_\pi^2}\,\zeta_4 + \Big(\frac{M g_A^2}{8\pi f^2}\Big)^2 \frac{M}{4\pi}\;\frac{m_\pi^2}{\gamma}\left[\mathrm{Re\,Li}\Big(\frac{-m_\pi}{m_\pi + 2\gamma}\Big) + \frac{\pi^2}{12}\right] \\ &= \frac{\gamma^2}{m_\pi^2}\,\zeta_4 + \Big(\frac{M g_A^2}{8\pi f^2}\Big)^2 \frac{M m_\pi}{4\pi}\left[2\ln 2 - (1 + 2\ln 2)\frac{\gamma}{m_\pi} + \mathcal{O}\Big(\frac{\gamma^2}{m_\pi^2}\Big)\right]\,. \end{aligned} \tag{12}$$

Since ζ_4 is multiplied by γ^2/m_π^2, this condition basically fixes the value of ζ_3. At this order ζ_1 may change from its value at NLO. We have chosen to fix ζ_1 and ζ_4 by performing a least square fit to the lower momentum data.

The ${}^1S_0$ phase shift is shown in Fig. 7. The solid line is the result of the Nijmegen phase shift analysis[29]. The ${}^1S_0$ phase shift has an expansion in

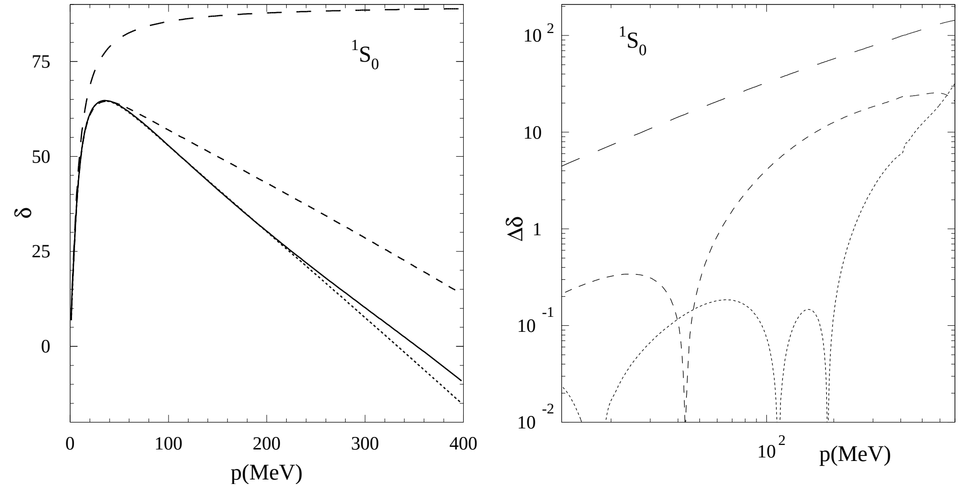

Figure 7: Fit to the $^1S_0$ phase shift δ emphasizing the low momentum region. The solid line is the Nijmegen fit [29] to the data (for $p > 400\,\mathrm{MeV}$ values from the VPI [30] phase shift analysis were used.). The long dashed, short dashed, and dotted lines are the LO, NLO, and NNLO results respectively. $\Delta\delta$ is the difference between these results and the solid line.

powers of Q, and we have plotted the LO, NLO and NNLO results. The LO phase shift at $p \sim m_\pi$ is off by 49%. At NLO, the error is 14%. At NNLO, the error in the $^1S_0$ channel is less than 2% at $p \sim m_\pi$, and the NNLO result gives improved agreement with the data even at $p \sim 400\,\mathrm{MeV}$.

Using $M = 939\,\mathrm{MeV}$ and $m_\pi = 137\,\mathrm{MeV}$, the parameters for our fit in the $^1S_0$ channel are:

$$\begin{array}{lllll} \mathrm{NLO}: & \zeta_1 = 0.2163; & \zeta_2 = 0.0318; & & \\ \mathrm{NNLO}: & \zeta_1 = 0.0777; & \zeta_2 = 0.0313; & \zeta_3 = 0.1831; & \zeta_4 = 0.2447; \end{array}$$

Note that $\zeta_3 \sim Q$ is larger than $\zeta_2 \sim Q^0$ because from Eqs. (11) and (12), $\zeta_3/\zeta_2 \sim m_\pi^2/(\gamma\Lambda_{NN})$. The parameter ζ_2 is stable because it is fixed by the NLO good fit condition. On the other hand, ζ_1 changes by a factor of 2.7 going from NLO to NNLO. One expects the value of coupling constants to change at each order in the expansion, but a factor of three difference is somewhat surprising. It is also disturbing that ζ_4 is greater than ζ_1, since, on the basis of the RGE, it is expected that $\zeta_4 < \zeta_1$. At NNLO the RGE for C_2 is: [4]

$$\mu\frac{\partial}{\partial\mu}C_2 = 2\frac{M\mu}{4\pi}\left(C_0 + \frac{g_A^2}{2f^2}\right)C_2\,.$$

Expanding C_2 perturbatively results in two equations:

$$\mu\frac{\partial}{\partial\mu}C_2 = 2\frac{M\mu}{4\pi}\,C_0\,C_2\,, \tag{13}$$
$$\mu\frac{\partial}{\partial\mu}C_{2,-1} = 2\frac{M\mu}{4\pi}\left[\left(C_{0,0}+\frac{g_A^2}{2f^2}\right)C_2 + C_0\,C_{2,-1}\right]\,,$$

with solutions

$$C_2 = \zeta_1\,C_0^2\,, \qquad C_{2,-1} = 2\frac{C_2}{C_0}\left(C_{0,0}+\frac{g_A^2}{2f^2}\right) + \zeta_4\,C_0^2\,. \tag{14}$$

The second term in $C_{2,-1}$ has exactly the same form as the leading C_2. $C_{2,-1}$ is supposed to be a perturbative correction to C_2, so $\zeta_4 \sim Q < \zeta_1 \sim Q^0$, and one does not expect this part of $C_{2,-1}$ to be significantly larger than the leading C_2.

Some insight into this puzzle can be obtained by comparing the NLO and NNLO expressions for r_0. Using Eq. (9) we have

$$\begin{aligned} r_0^{NLO} &= \frac{8\pi}{M}\zeta_1 + \frac{2}{\Lambda_{NN}}\left(1-\frac{8\gamma}{3m_\pi}+\frac{2\gamma^2}{m_\pi^2}\right) \\ &= \frac{8\pi}{M}(\zeta_1 + 0.2952)\,, \qquad (15) \\ r_0^{NNLO} &= \frac{8\pi}{M}\left[\zeta_4 + \zeta_1\left(1-\frac{2m_\pi-2\gamma}{\Lambda_{NN}}\right) + \frac{\zeta_2}{\Lambda_{NN}}\left(\frac{8m_\pi}{3}-4\gamma\right)+\ldots\right] \\ &= \frac{8\pi}{M}(\zeta_4 + 0.01375\,\zeta_1 + 1.35078\,\zeta_2 + 0.210398)\,, \qquad (16) \end{aligned}$$

where $1/\Lambda_{NN} = (Mg_A^2)/(8\pi f^2)$. Any reasonable fit for the phase shifts will at least approximately reproduce the observed effective range. In Eq. (16), the piece of the NLO correction proportional to ζ_1 is almost exactly cancelled by the NNLO correction. This cancellation occurs because $1-2(m_\pi-\gamma)/\Lambda_{NN} \simeq 0.01$ in the $^1S_0$ channel. This is simply an unfortunate accident; in the $^3S_1$ channel, where $\gamma = 45.7\,\mathrm{MeV}$ instead of $-7.88\,\mathrm{MeV}$, the coefficient of ζ_1 in Eq. (16) is ≈ 0.4. Since ζ_2 is small due to the NLO good fit condition, this accidental cancellation forces ζ_4 to make up the observed effective range. Therefore, ζ_4 is much larger than anticipated.

It is important to note that the coupling C_2 is not changing nearly as drastically at each order. If one were to solve the theory exactly, one would find that C_2 had a term $\hat{r}\,C_0^2$, where $\hat{r}$ represents a short distance contribution to the effective range. ζ_1 and ζ_4 can be thought of as the first few terms in an expansion of $\hat{r}$. The theory should eventually converge to the exact $\hat{r}$ but it need not reproduce $\hat{r}$ exactly at low orders in perturbation theory. It is reassuring that $\zeta_1^{NLO} = 0.22$ and $\zeta_1^{NNLO} + \zeta_4^{NNLO} = 0.32$, indicating that the coupling constant C_2 is not changing more than one would expect in a theory with an expansion parameter $\sim 1/3$. Note that ζ_1^{NNLO} must be small in order for $\zeta_1^{NNLO} + \zeta_4^{NNLO}$ to not be much larger than ζ_1^{NLO}. At NLO potential pions make up $\sim 60\%$ of r_0, with short distance physics making up the remaining $\sim 40\%$. At NNLO the situation does not change by very much; potential pions give $\sim 40\%$, short distance physics $\sim 50\%$ and cross-terms make up the rest.

Kaplan and Steele[28,31] have proposed a fitting procedure in which $\hat{r}$ is not expanded in powers of Q. This amounts to imposing the additional condition $\zeta_4 = 0$, so there is no new parameter at NNLO. Only the linear combination $\zeta_1 + \zeta_4$ appears in C_2. However the amplitude depends on ζ_1 and ζ_4 very differently because they appear at different orders in the Q expansion. This is why we treat ζ_1 and ζ_4 as seperate parameters. Where it not for the cancellation in r_0^{NNLO} noted above, then the difference between the two methods would be small, i.e., the size of a N^{3}LO correction. In fact, it is impossible to reproduce the observed effective range if one demands $\zeta_4 = 0$. In the $^3S_1$ channel their is a logarithmic divergence[4] at order Q, introducing a $\ln(\mu/K)$ dependence into the coupling $C_{2,-1}$. Since the constant K is undetermined, ζ_4 cannot be set to zero, so there is a new parameter at NNLO. For C_2^S this type of $\ln(\mu)$ dependence occurs at order Q^2 from soft pion graphs.[16] Kaplan and Steele have suggested that the failure of their fitting procedure when applied to models with effective ranges close to that seen in nature may indicate that r_0 is unnaturally large, and that the power counting of the effective theory might need to be modified to take this scale into account. It seems more likely that the failure observed in Ref. [31] may just be the consequence of a numerical accident in the amplitude at NNLO as shown in Eq. (16). This cancellation does not occur in the $^3S_1$ channel at NNLO, nor is it likely to persist at higher orders. For this reason, it seems premature to conclude on the basis of the NNLO amplitude that the expansion is failing due to a large r_0.

In Ref. [20], Rupak and Gautam use a similar fitting procedure to the one discussed here. Instead of finding ζ_1 and ζ_4 by fitting to the phase shift, they fix these constants by matching onto

$$p\,\cot(\delta) = -\gamma + \frac{s_0}{2}\,(p^2 + \gamma^2) + \dots\,, \tag{17}$$

which is similar to the effective range expansion except $p\cot(\delta)$ is expanded about $p = i\gamma$. At NLO ζ_1 is fixed to give s_0. At NNLO the same value of ζ_1 is used and ζ_4 is again fixed to reproduce s_0. This procedure was applied to data from a two-Yukawa toy model and the convergence of the EFT looks similar to that in Fig. 7. In our approach we have not demanded that the exact value of r_0 is reproduced since we know that there will be corrections to r_0 from higher orders in the m_π/Λ expansion.

Finally, we would like to comment on the prediction of higher order terms in the effective range expansion

$$p\cot(\delta) = -\frac{1}{a} + \frac{r_0}{2}p^2 + v_2 p^4 + v_3 p^4 + v_4 p^4 \ldots .$$

Using the NLO expression for $p\cot(\delta)$, Cohen and Hansen[32] obtained predictions for v_2, v_3 and v_4. At NLO, the effective field theory predictions for v_2, v_3, and v_4 disagree with the v_i obtained from a fit to the Nijmegen phase shift analysis. The NNLO predictions for the shape parameters are shown in the table below. The prediction for r_0 is not better at NNLO than at NLO. The NNLO v_i predictions depend on ζ_1 and ζ_2. We see that the NNLO correction substantially reduces the discrepancy between the effective field theory prediction and the fit to the Nijmegen phase shift analysis, but the discrepancy is still quite large. This gives some evidence that the EFT expansion is converging on the true values of the v_i, albeit slowly. Effective field theory predictions for the shape parameters have been studied in toy models where one is able to go to very high orders in the Q expansion.[33] In the toy models, the effective field theory did eventually reproduce the shape parameters, but the observed convergence is rather slow.

$^1S_0$		r_0	v_2	v_3	v_4
	Fit[32]	2.73 fm	$-0.48\,\mathrm{fm}^3$	$3.8\,\mathrm{fm}^5$	$-17\,\mathrm{fm}^7$
	NLO	2.65 fm	$-3.3\,\mathrm{fm}^3$	$19\,\mathrm{fm}^5$	$-117\,\mathrm{fm}^7$
	NNLO	2.63 fm	$-1.2\,\mathrm{fm}^3$	$2.9\,\mathrm{fm}^5$	$-0.7\,\mathrm{fm}^7$

What can we learn from Fig. 7 about the convergence of the KSW expansion? It is pleasing to see a NNLO calculation reproducing the $^1S_0$ phase shift at $p \sim m_\pi$ with an accuracy of a few percent, and giving an improved fit to the data even for larger momenta. It is important to keep in mind that the NNLO calculation of the phase shift is incomplete since there is a possible contribution from order Q_r^4 radiation pion graphs. Many other process involving two nucleons can be examined at this order. Once enough processes are calculated to NNLO, all parameters of the theory appearing at this order can be extracted and it will be possible to make predictions with no free parameters. The accuracy of these predictions will constitute a serious test of the KSW expansion method.

Acknowledgments

We would like to thank D. Kaplan, G. Rupak, and N. Shoresh, for useful discussion. This work was supported in part by the Department of Energy under grant number DE-FG03-92-ER 40701. T.M. was also supported by a John A. McCone Fellowship.

Appendix

Here we give the definitions of the constants appearing in the NNLO expression for the amplitude in Eq. (9). After solving the renormalization group equations at this order one finds that all quantities in parentheses and curly brackets are separately μ independent. The quantities in curly brackets vanish at NNLO in the Q expansion.

$$
\begin{aligned}
\gamma &= \frac{4\pi}{MC_0} + \mu \; ; \qquad \zeta_1 = \left(\frac{C_2}{C_0^2}\right) ; \\
\zeta_2 &= \left(\frac{D_2}{C_0^2} - \frac{g_A^2}{4f^2}\Big(\frac{M}{4\pi}\Big)^2 \left[1 + \ln\Big(\frac{\mu^2}{m_\pi^2}\Big)\right]\right) + \left(\frac{g_A^2/(2f^2) + C_{0,0}}{C_0^2\, m_\pi^2}\right) ; \\
\zeta_3 &= -\frac{g_A^2}{2f^2}\frac{Mm_\pi}{4\pi}\left(\frac{C_2}{C_0^2}\right) + \frac{1}{m_\pi^2}\left(\frac{C_{0,1}}{C_0^2} - \frac{[g_A^2/(2f^2) + C_{0,0}]^2}{C_0^3}\right) \\
&\quad + m_\pi^2 \left\{\frac{D_4}{C_0^2} - \frac{D_2^2}{C_0^3}\right\} + \left(\frac{D_{2,-1}}{C_0^2} - \frac{2D_2[g_A^2/(2f^2) + C_{0,0}]}{C_0^3} + \frac{g_A^2}{2f^2}\frac{\mu M}{4\pi}\frac{C_2}{C_0^2}\right) \\
&\quad + \left(\frac{\Delta D_2(\mu)\, m_\pi^2}{C_0(\mu)^2} - 6\,\frac{g_A^2 m_\pi^2}{(4\pi f)^2}\,\frac{M}{4\pi}\Big(\frac{1}{a^S} - \frac{1}{a^T}\Big)\left[\frac{1}{3} + \ln\Big(\frac{\mu^2}{m_\pi^2}\Big)\right]\right) ; \\
\zeta_4 &= \left(\frac{C_{2,-1}}{C_0^2} - \frac{2\, C_2\, [g_A^2/(2f^2) + C_{0,0}]}{C_0^3}\right) + m_\pi^2 \left\{\frac{E_4}{C_0^3} - \frac{2\, C_2\, D_2}{C_0^2}\right\} ; \\
\zeta_5 &= m_\pi^2 \left\{\frac{C_4}{C_0^2} - \frac{C_2^2}{C_0^3}\right\} .
\end{aligned}
\tag{18}
$$

ζ_1 and ζ_4 are short distance constants of integration of the RGE's in Eq. (13). On the other hand, ζ_2 and ζ_3 are sums of constants and variables that appear in the amplitude. Note that the order Q radiation pion contribution from order Q_r^3 graphs is constant and appears in ζ_3. $\Delta D_2(\mu)$ is a correction to D_2 which cancels the $\ln(\mu)$ dependence from the Q_r^3 radiation pion graphs.

References

1. D.B. Kaplan, M.J. Savage, and M.B. Wise, *Phys. Lett.* **B**424 (1998) 390.

2. D.B. Kaplan, M.J. Savage, and M.B. Wise, *Nucl. Phys.* **B**534 (1998) 329.
3. J. Gegelia, nucl-th/9802038; T. Mehen, and I. Stewart, Phys. Lett. **B445** (1999) 378.
4. T. Mehen and I. Stewart, Phys.Rev. C59 (1999) 2365.
5. G.P. Lepage, nucl-th/9706029.
6. J. Steele, *talk presented at this workshop*, nucl-th/9904023.
7. E. Epelbaum and U-G. Meissner, *talk presented at this workshop* nucl-th/9903046; nucl-th/9902042.
8. X. Kong and F. Ravndal, hep-ph/9903523, *Phys. Lett.* **B450** (1999) 320.
9. D.B. Kaplan, M.J. Savage, and M.B. Wise, *Phys. Rev.* **C**59 (1999) 617.
10. J.W. Chen, H.W. Greisshammer, M.J. Savage and R.P. Springer, *Nucl. Phys.* **A644** (1999) 221.
11. X. Kong and F. Ravndal, nucl-th/9904066, nucl-th/9902064.
12. M.J. Savage, K.A. Scaldeferri and M.B. Wise, nucl-th/9811029; D.B. Kaplan, M.J. Savage, R.P. Springer and M.B. Wise, *Phys. Lett.* **B449** (1999) 1; J.-W. Chen, G. Rupak and M.J. Savage, nucl-th/9905002.
13. J.W. Chen, H.W. Greisshammer, M.J. Savage and R.P. Springer, *Nucl. Phys.* **A644** (1999) 245; J.-W. Chen, nucl-th/9901012.
14. M. Butler, and J.W. Chen, nucl-th/9905060.
15. M.J. Savage, *talk presented at this workshop*, nucl-th/9905009.
16. T. Mehen and I.W. Stewart, nucl-th/9901064.
17. T. Mehen, I.W. Stewart, and M.B. Wise, hep-ph/9902370.
18. M.B. Wise, *talk presented at this workshop*, nucl-th/9904509.
19. G. Rupak, *talk presented at this workshop.*
20. G. Rupak and N. Shoresh, nucl-th/9902077.
21. M. Neubert, *Phys. Rep.* **245**, 259 (1994).
22. H.W. Griesshammer, *Phys. Rev.* **D58** (1998) 094027; hep-ph/9810235.
23. M. Beneke and V.A. Smirnov, *Nucl. Phys.* **B522** (1998) 321.
24. S.G. Gorishny, *Nucl. Phys.* **B319** (1989) 633; G.B. Pivovarov and F.V. Tkachov, *Int. Journ. Mod. Phys.* **A8** (1993) 2241; V.A. Smirnov, *Phys. Lett.* **B394** (1997) 205; A. Czarnecki and V.A. Smirnov, *Phys. Lett.* **B394** (1997) 211; V.A. Smirnov and E.R. Rakhmetov, hep-ph/9812529.
25. K.G. Chetyrkin, Teor. *Mat. Fiz.* **75** (1998) 26; *ibid* **76** (1998) 207; K.G. Chetyrkin and V.A. Smirnov, *Phys. Lett.* **B144** (1984) 419; V.A. Smirnov, *Commun. Math. Phys.* **134** (1990) 109; V.A. Smirnov, *Renormalization and asymptotic expansions*, Birkhäuser, Basel, 1991.
26. S. Fleming, T. Mehen and I.W. Stewart, *work in progress.*
27. J.-W. Chen, G. Rupak and M. J. Savage, nucl-th/9902056.

28. D.B. Kaplan, *talk presented at this workshop.*
29. V.G.J. Stoks, et.al., Phys. Rev. **C48** (1993) 792; V.G.J. Sto ks et.al., Phys. Rev. **C49** (1994) 2950, nucl-th/9406039. (cf. http://nn-online.sci.kun.nl/NN/)
30. R. A. Arndt and R. L. Workman, Few Body Syst. Suppl. 7 (1994) 64; Data from: http://said.phys.vt.edu/
31. J. Steele and D.B. Kaplan, nucl-th/9905027.
32. T.D. Cohen and J.M. Hansen, Phys. Rev. **C59** (1999) 13; nucl-th/9901065. T.D. Cohen, *talk presented at this workshop.*
33. D.B. Kaplan, *private communication*